

We are IntechOpen, the world's leading publisher of Open Access books Built by scientists, for scientists

6,900

Open access books available

186,000

International authors and editors

200M

Downloads

Our authors are among the

154

Countries delivered to

TOP 1%

most cited scientists

12.2%

Contributors from top 500 universities



WEB OF SCIENCE™

Selection of our books indexed in the Book Citation Index
in Web of Science™ Core Collection (BKCI)

Interested in publishing with us?
Contact book.department@intechopen.com

Numbers displayed above are based on latest data collected.
For more information visit www.intechopen.com



Construction of Drug Screening Cell Model and Application to New Compounds Interfering Production and Accumulation of Beta-Amyloid by Inhibiting Gamma-Secretase

Xiao-Ning Wang¹, Jie Yang¹, Ping-Yue Xu¹,
Jie Chen^{1,2}, Dan Zhang¹, Yan Sun¹ and Zhi-Ming Huang¹

¹*State Key Laboratory of Pharmaceutical Biotechnology, Department of Biochemistry,
College of Life Sciences, Nanjing University, Nanjing 210093,*

²*Department of Pathology, The University of Hong Kong,
Queen Mary Hospital, Pokfulam Road,*

¹*P.R.China*

²*Hong Kong*

1. Introduction

Alzheimer's disease (AD) is a tenacious neurodegenerative dementia, characterized clinically by progressive loss of memory, cognitive dysfunction, and behavioral abnormalities, accompanied by the accumulation of intracellular neurofibrillary tangles (NFTs), neuropil threads, as well as extracellular amyloid-beta containing senile plaques, cerebrovascular amyloid-beta deposits, and selective nerve cell and synapse loss (Kelliher et al, 1999; Tanzi, 1999; Solerte et al, 2000). The last two decades have witnessed an expanding body of research that elucidated the central role of amyloid precursor protein (APP) processing and amyloid beta (Abeta) production in the risk, onset, and progression of AD (Findeis, 2007). The accumulation of insoluble aggregates of Abeta peptide 1-42 (Abeta42) derived from APP is believed to play an important role in AD (Hardy, 1997; Kelliher et al, 1999). The generation of Abeta peptides requires two sequential proteolytical cleavages of APP by beta-secretase (BACE1) (Roßner et al, 2006) and gamma-secretase, composed of four integral membrane proteins, presenilins (PS1/2), APO-1 (anterior pharynx-defective 1), PEN-2 (presenilin enhancer 2) and nicastrin (NCT) (Kaether et al, 2006; Zhang & Koo, 2006). Previous evidence points to the involvement of the endoplasmic reticulum (ER) in AD pathogenesis owing to the fact that it is an important site for generating Abeta42 in neurons (Hartmann et al, 1998) and that presenilins are predominantly localized in this cellular compartment (Kovacs et al, 1996; Cook et al, 1996). Cleavage of the APP ectodomain by beta-secretase at the amino-terminus of Abeta is followed by cleavage of the beta-secretase-generated carboxyl-terminal fragment (beta-CTF, C99) at the carboxyl terminus of Abeta by gamma-secretase. A third activity, referred to as alpha-secretase, cleaves otherwise the APP ectodomain within the Abeta sequence, and subsequent cleavage of the alpha-secretase-derived APP CTF (alpha-CTF, C83) by gamma-secretase results in production of P3

(Abeta17-40/42) (McLendon, et al., 2000; Roßner et al, 2006; Walsh, et al., 2007). Studies in molecular pathology have indicated that the accumulation of Abeta leads to Abeta fibril deposition or beta-sheet amyloid deposition, whereas the dye molecular Congo red can interfere with beta-amyloid fibril formation as well as bind to preformed fibrils and prevent in vitro cytotoxicity, which is supported by the results of Carter DB and Chou KC (1998).

On the other hand, nicotine produces its actions on mammalian tissue via interactions with a family of ligand-gated ion channels that modulate the effects of the alkaloid on nervous, cardiovascular, immune, and neuromuscular system function (Wei, et al, 2005). The neuronal nicotinic acetylcholine receptors (nAChRs) are named on the basis of their subunit components and are thought to have a pentameric functional motif formed from a variety of subunits that comprise an ion channel similar to that of the neuromuscular junction nAChR. Two of the most abundant brain nAChRs are the heteromeric alpha4beta2 and homomeric alpha7 subtypes and the latter is an important target for Abeta-mediated neurotoxicity (Wang, et al, 2000). Abeta42 activation of alpha7 receptors expressed in the *Xenopus laevis* oocyte was prevented by two alpha7 ligands, the antagonist methyllycaconitine and a metabolite of GTS-21 (Wei, et al, 2005). The alpha7 receptor agonists enhance cognition and auditory-gating processes and thus are attractive drug candidates for the treatment of senile dementias and schizophrenia. Chou KC group has screened and found new drug candidates for treating Alzheimer's disease using GTS-21 as a template to search the Traditional Chinese Medicines Database by DOCK module based on the structure of alpha7 nicotinic acetylcholine receptor (Wei, et al, 2005). In addition, a key hallmark for AD is the decreased level of acetylcholine, a neurotransmitter playing a decisive role in memory and learning (Whitehouse, et al, 1982). Acetylcholinesterase (AChE), which degrades acetylcholine to its inactive metabolite choline, has emerged as a promising target for the management of AD. We have characterized some novel poly-phenols from the stem bark of *Hopea hainanensis*, especially hopeahainol A as AChE inhibitors with an IC₅₀ value of 4.33 µM (Ge, et al, 2008). We have even made progress with the interaction between AD-related proteins and other proteins focused attention upon as potential drug targets (Jiang, et al, 2006). Moreover, the identification of the cell type-specific expression and activation of NF-kB, Sp1 and YY1 transcription factors may provide a basis to specifically interfere with BACE1 expression and, thereby, to lower the concentrations of Abeta peptides, which may prevent neuronal cell loss and cognitive decline in AD patients (Roßner et al, 2006).

It is clear that the accumulation of Abeta initiates a series of downstream neurotoxic events. As a result, considerable attention is being focused on attempts to develop therapies for Alzheimer's disease that are directed towards metabolic pathways that involve Abeta. One way is to reduce production of Abeta through the upstream processing enzymes (beta-secretase and gamma-secretase). gamma-secretase is a multi-subunit protease complex, minimally consists of four individual proteins: presenilin, nicastrin, APh-1, and PEN-2. Consequently, several gamma-secretase inhibitors have recently been described, including transition state analogs that mimic the gamma-secretase cleavage site on the immediate Abeta precursor (C99) and presumably compete with it for binding to the gamma-secretase enzymatic site (Netzer, et al., 2003). Here express gamma-secretase's substrate (such as EGFP-tagged C99 of APP) in the cultured cells (CHO) under control of tetracycline inducible system (Tet-off system) and then evaluate the efficiency of the inhibitors by ELISA (Enzyme-Linked Immunosorbent Assay) and Western blot. This paper focuses on construction of a drug screen model for AD's gamma-secretase inhibitors and further finds some active compounds possessing gamma-secretase inhibition activity.

2. Materials and methods

2.1 Materials

The expression plasmids pcDNA3.1 (-), pEGFP, T vector (pBluescript II SK (+)), and tetracycline inducible expression system (pUHD30F and p15-1neo) were kindly provided by Prof Xue-Liang Zhu (Institute of Biochemistry and cell Biology, Chinese Academy of Sciences). The restriction endonucleases, SacII, XbaI, EcoRI, BamHI, HindIII and Cfr9I, and T4 DNA ligase were purchased from MBI Ferments (MD, USA). NdeI, SacI, XbaI, BspE I (AccIII) and ExTaq polymerase were obtained from TAKARA Bio Inc. Taq DNA polymerase and Pfu-Taq DNA polymerase were purchased from Shanghai Bioasia Biotechnology Co., Ltd (China). UNIC-10 trizol total RNA extraction kit, RT-PCR kit, DNA gel extraction kit, Uniq-10 DNA retraction kit, and plasmid mini preparation kit were from Shanghai Sangon Biotechnology Company (China). Methylenebisacrylamide, acrylamide, BSA, EDTA, and standard molecular weight protein marker were purchased from Nanjing Shengxing Biotechnology Co., Ltd (China). DNA marker was from MBI Company. The primers for PCR were synthesized by Shanghai Bioasia Biotechnology Co., Ltd (China).

The Chinese hamster cell lines CHO (ATCC 9096) was kindly provided by Prof Xue-Liang Zhu (Institute of Biochemistry and cell Biology, Chinese Academy of Sciences). Transfast™ reagent (eukaryotic cell transfection kit) was obtained from Promega Company (Madison, WI., USA). DMEM (Dulbecco's Modified Eagles' Medium) was obtained from GIBCO. New Zealand fetal bovine serum (FBS), L-glutamine, Trypsin, sodium pyruvate, ampicillin (Amp), and aminoglycosides (i.e. neomycin and kanamycin) were purchased from Hyclone (Logan, UT, USA). G418 (geneticin) was obtained from Ameresco Inc. PC152 (anti-beta-amyloid (15-30) rabbit pAb), recognizing three beta-amyloid peptides (Abeta40, Abeta42, and Abeta43), was obtained from Merck Co. Inc. Bovine insulin, bovine GSA (G-protein's alpha), and 3-(4,5-dimethylthiazol-2-yl)-2,5-diphenyltetrazolium bromide (MTT), and were obtained from Sigma Co. (St. Louis, MO, USA). BCA (bicinchoninic acid), ELISA TMB (3,3',5,5'-tetramethylbenzidine), PBS buffer (PH7.4), Hepes, CaCl₂, Na₂HPO₄, and NaH₂PO₄ were purchased from Shanghai Sagon Company (China). 2-substituted-1,2,3,4-tetrahydro-isoquinoline derivatives (compound **I1-I6** and **II1-II6**) were designed and synthesized by our laboratory.

2.2 Design and construction of expression plasmids

2.2.1 Construction of expression plasmid pcDNA-C99 of human APP segment

Human total RNA was extracted from brain using UNIC-10 trizol total RNA extraction kit. Then obtain cDNA by reverse transcription using RT-PCR kit. C99 includes gamma-secretase active sites as gamma-secretase substrate. Taking cDNA as a template, the region of the gene encoding C99 of human APP (Homo sapiens amyloid beta (A4) precursor protein, NM_000484) was amplified by PCR using the following oligonucleotides: 5'-GCT GGATCC gcagaattccgacatgactc-3' as the 5' forward primer and 5'-AGC AAGCTT ctagtctgcatctgctcaaag-3' as the 3' reverse primer (restriction sites for BamHI and HindIII are underlined, respectively) according to Goo and Park (2004). The PCR product was purified using agarose gel DNA extraction kit and confirmed by sequencing analysis. The sequencing analysis is consistent with the gene sequence (1986-2282) of human APP (NM_201414.1), which codes residue 661-759 segment of human APP (NM_201414.1), namely residue 672-770 of APP770 (Fig. 1a). The PCR product was restricted with BamHI and HindIII, identified by 10g/L agarose gel electrophoresis and cloned into expression

vector pcDNA3.1(-), named pcDNA-C99. The expression vector was transformed into Escherichia coli DHalpha5 fertilized on LB (30µg /ml Amp included) plate at 37°C overnight for amplification screening. Single clone was selected to be cultured in LB liquid overnight and then purified using plasmid mini preparation kit. The expression vector was verified by PCR, digestion and sequencing (Fig. 1b).

1 MLPGLALLLL AAWTARALEV PTDGNAGLLA EPQIAMFOGR LNMHMNVQNG KMDSDPSGTK
61 TCIDTKEGIL QYCQEVYPEL QITNVVEANQ PVTIQNWCKR GFKQCKTHPH FVIPYRCLVG
121 EFVSDALLVP DKCKFLHQR MDVCETHLHW HTVAKETCSE KSTNLHDYGM LLPCGIDKFR
181 GVEFVOCPLA EESDNVDSAD AEEDDSVMMW GGADTDYADG SEDKWEVAE EEEVAEVEEE
241 EADDDDEDDED GDEVEEEAEE PYEEATERIT SIATTTTTTT ESVEEVREV CSEQAETGPC
301 RAMISRMYFD VTEGKCAPFF YGGCGGNRNN FDTEEYCMAY OGSAMSQSLL KTTQEPLARD
361 PVKLPTTAAS TPDVVDKYLE TPGDENEHAH FQKAKERLEA KHRERMSQVM REMEEAERQA
421 KNLPKADKKA VIQHFQEKVE SLEQEAANER QQLVETHMAR VEAMLNDRRR LALENYITAL
481 QAVPPRPRHV FNMLKKYVRA ECKDRQHTLK HFEHVRMVDP KKAQIRSQV MTHLRVIYER
541 MNQSLSLLYN VPAVAEEIQD EVDELLQKEQ NYSDDVLANM ISEPRISYGN DALMPSLTET
601 KTTVELLPVN GEFSLDDLQP WHSFGADSV ANTENEVEPV DARPAADRGL TTRPGSGLTN
661 IKTEEISEVK MDAEFRHDSG YEVHHQKLVF FAEDVGSNKG AIIGLMVGGV VIATVIVITL
721 VMLKKKQYTS IHHGVVEVDA AVTPEERHLS KMQQNGYENP TYKFFEQMQN

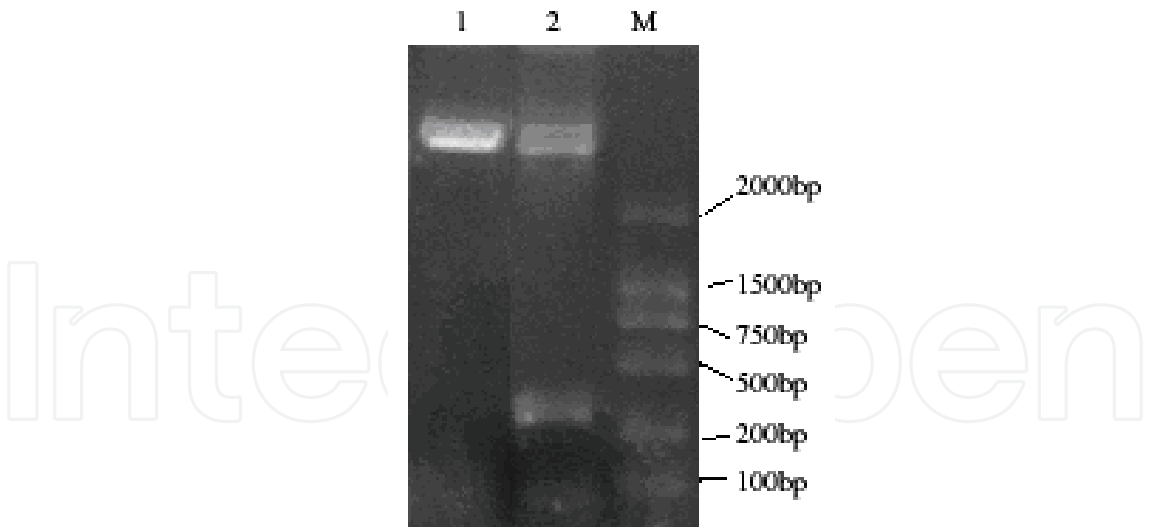


Fig. 1. Amino acid sequence of APP770, in which the single-underlined amino acid sequence means APP695. a) The amino acid sequence double-underlined displays Abeta42, while that shaded (D₆₇₂-N₇₇₀) figures C-terminal fragment of APP of 99 amino acids (C99, including gamma- secretase active sites). b) Southern blot of recombinant APP fragment by Agarose gel electrophoresis. Note: 1. Empty pcDNA3.1(-); 2. Not digested pcDNA3.1(-)-C99; M. DNA Marker. C99 gene fragment is about 300bp. DNA marker are 100, 200, 500, 750, 1000 and 2000bp

2.2.2 Construction of LGC (leading peptide -EGFP-C99) fusion gene

Construction of LGC fusion gene was based on APP leading peptide, pEGFP-C1, and pcDNA-C99, which is able to express a EGFP-tagged C99 segment under control of the tetracycline-responsive system (Zhu, 1999). Schematic diagrams of all constructs are shown in Fig. 2A. To construct pLGC, the region coding for APP leading peptide, containing nucleotides 195 to 245 (NM_201414_1), was synthesized as the 5' forward primer of LGC fusion; the region coding for EGFP was from pEGFP-C1 (Clontech); and the region coding for C99 was from pcDNA-C99. To link EGFP to C99, BspE I (AccIII or BspM II) restriction site was introduced into 3' reverse primer of EGFP and 5' forward primer of C99, respectively. To render membrane localization of LGC fusion produced by pLGC, a sequence coding for APP's signal peptide (nucleotides 195 to 245) was introduced in frame into the *NheI* site located before the EGFP-coding sequence and C99 cDNA to form pLGC-EGFP. The region of the gene encoding APP's leading peptide-EGFP fusion segment (LG) was amplified by PCR with primers: 5'-GTGCTAGC atgctgcccggtttggcactgctcctgctggccgctggacggctcgggcgctggaggtaccact gatatggtgagcaagggcgaggag-3' as the 5' forward primer and 5'-GATCCGGA ctgtacagctcgtccatgc-3' as the 3' reverse primer (restriction sites for *NheI* and *BspEI* are capital letters underlined, respectively, while the signal peptide of APP is small letters underlined). The PCR fragment was cleaved with *NheI* and *BspE I* and then was ligated to replace the *NheI*-*BspEI* restriction fragment of pEGFP-C1 (nucleotides 592 to 1330). Similarly, the encoding region of C99 was amplified by PCR using the following oligonucleotides: 5'-GCTCCGGA gcagaattccgacatgactc-3' as the 5' forward primer and 5'-AGCAAGCTT ctagttctgcatctgctcaaag-3' as the 3' reverse primer (restriction sites for *BspEI* and *HindIII* are underlined, respectively). The PCR fragment was digested with *BspE I* and *HindIII* and then was ligated to replace the *BspEI*-*HindIII* restriction fragment of pEGFP-C1 (nucleotides 1331 to 1352). The resulting plasmid was named pLGC-EGFP. The PCR fragment in pLGC-EGFP was sequenced. The sequence coding for the 17-residue leading peptide of APP was inserted as previously described. pLGC-EGFP was constructed from pEGFP-C1 to express LGC fusion with a signal peptide at N termini as in APP.

Then, the region of the gene encoding LGC fusion segment was amplified by PCR using the following oligonucleotides: 5'-CCTCCGCGG atgctgcccgggtttggcactg-3' as the 5' forward primer and 5'-TCCTCTAG actagttctgcatctgctcaaag-3' as the 3' reverse primer (restriction sites for *SacII* and *XbaI* are underlined, respectively). The PCR product was restricted with *SacII* and *XbaI*; the resultant ~ 1.1kb fragment was ligated to replace the *SacII*-*XbaI* fragment of pUHD30F, a vector derived from pUHD20 (Zhu et al, 1997), to create pLGC-30F. The PCR fragment in pLGC-EGFP was sequenced and identified by 10g/L agarose gel electrophoresis.

The expression vectors (pLGC-EGFP and pLGC-30F) was transformed into *Escherichia coli* DHalpha5 fertilized on LB (30μg /ml Amp included) plate at 37°C overnight for amplification screening. Picked monoclonal to amplify, extracted plasmids, and tested positive clones by PCR, enzymatic detection, and sequencing of positive clones (Fig. 2).

- Construction of LGC fusion gene;
- Construction of expression plasmid pLGC-EGFP;
- Construction of tetracycline-inducible expression system (pLGC-30F);
- Southernblot of recombinant plasmid pLGC-EGFP (left) and pLGC-30F (right) by agarose gel electrophoresis. 1. DNA marker; DNA marker are 100, 250, 500, 750, 1000

and 2000bp. Left: 2-3. PCR analysis; 4-5. Digested pLGC-E by NheI and HindIII. Right: 2-3. Digested pLGC-30F by SacII and XbaI; 4-5. PCR analysis.

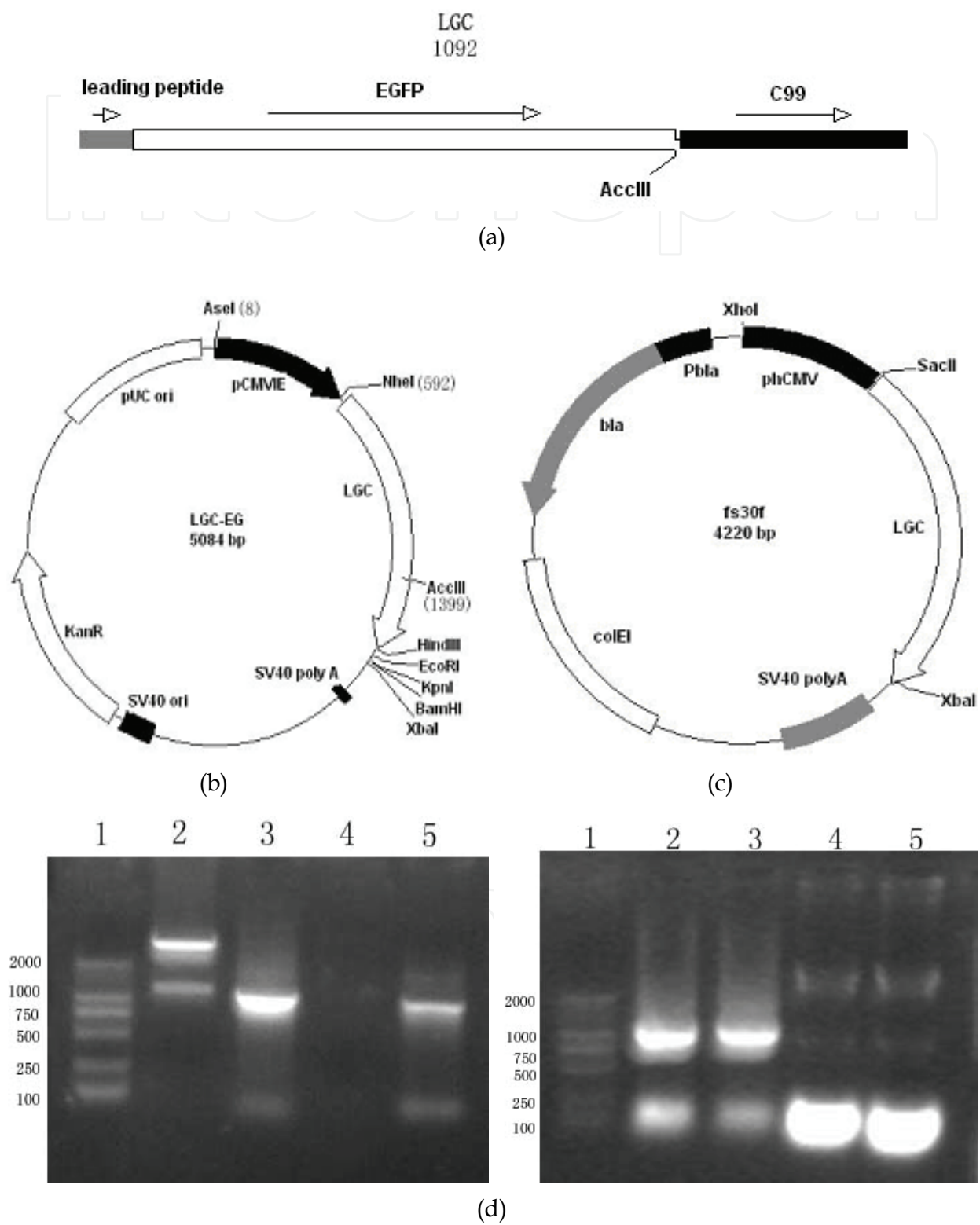


Fig. 2. Construction of LGC fusion gene and recombinant plasmids pLGC-EGFP and pLGC-30F

2.3 Stable expression of LGC fusion in CHO cells

2.3.1 Cell culture

Chinese hamster ovary (CHO) cells were cultured in a humidified atmosphere of 5% CO₂, 95% air at 37 °C with DMEM (Dulbecco's modified Eagle medium) growth media supplemented with 10% FBS, 3% glutamine and 20 µg/ml kanamycin (Basani et al., 2001; Basani et al., 2000; Pabón et al., 2006). After 7-10 days of culture, colonies with CHO morphology were passed to fresh feeder layers for subculture. Resulting colonies were dissociated for 10 min with 0.25% trypsin and passed to fresh feeder layers at 5-10-day intervals, depending on the proliferation rate. The CHO cell lines at a stage of rapid proliferation were chosen for the following transgenic experiment.

2.3.2 Transfection and selection of stably transfected cells under control of Tet-off system

Stable transfection of tTA into CHO cells was done via the calcium phosphate coprecipitation (CPP) method (Resnitzky et al, 1994; Zhu et al, 1997; Baron et al, 1997; Ryoo et al, 1997). For stable expression, CHO cells were transfected and selected with G418 as described previously (Yang et al, 2009). Briefly, CHO cells were incubated in 24-well plates at a density of 5.5×10^5 cells per well for 24 h before transfection. CHO cells were transfected with 20 µg of pLGC-30F in combination with 2 µg of p15-1neo (modified by P.L. Chen and W.-H. Lee by inserting a G418-resistant gene into p15-1, one of the two plasmids required for the tetracycline system) using the calcium phosphate method (Zhu et al, 1997). For transient expression, cells were assayed 48 h after transfection. Clones were selected in the presence of G418 (1 mg/ml), cells were extracted, and proteins were analyzed by sodium dodecyl sulfate (SDS)-polyacrylamide gel electrophoresis and then by immunoblotting with anti-amyloid monoclonal antibody (Resnitzky et al, 1994). Positive clone was found to induce expression from both plasmids in the absence of Tet and was chosen to be used in the subsequent experiments.

Cells were subsequently cultured in presence of G418 (1 mg/ml) for 3 weeks. We replenished the selective media every 3-4 days, and observed the percentage of surviving cells. Viable colonies were subcultured to test inducible expression of the EGFP-tagged C99 by ELISA, fluorescence assay and western blot analysis. Cells stably transfected with the empty pUHD-30F vector were selected with G418 and used as a control (Appendix 1). Tetracycline (1 µg/ml) was always included in the culture medium until expression of exogenous LGC fusion was required (Gossen and Bujard, 1992; Resnitzky et al, 1994). G418-resistant colonies were then cultured as a whole in DMEM containing 0.2 mg of G418/ml. To prevent unscheduled expression, all the transfected cells were maintained in DMEM containing tetracycline (1 mg/ml) (Zhu et al, 1997; Zhu, 1999). G418-resistant CHO colonies expressing LGC under control of tetracycline (tetracycline-inducible expression system, Tet-off system), named Tet-CHO.

2.3.3 ELISA using anti-beta-amyloid

2.0×10^5 cells were plated in 96-well plates and incubated with primary rabbit anti-beta-amyloid (15-30) antibody (PC152) (1:2000 dilution) in PBS buffer with 1% BSA followed by 10 mins incubation of HRP-conjugated goat anti-rabbit IgG (1:20000 dilution) in PBS buffer with 1% BSA. Optical density (OD) determined by ultraviolet spectrophotometry was measured with an ELISA plate reader at test wavelength of 450nm (table 1). Absorbance

value (A_{450}) was used for calculating cell survival rate as follows: survival rate=(A_{450} for experimental group/ A_{450} for control group) $\times 100\%$.

Clones	ELISA ^a										WB ^b		F-EGFP ^c
	1	2	3	4	5	6	7	8	9	Mean \pm S.D.	Anti-Abeta		Fluorescence
A (control)	0.0528	0.0550	0.0537	0.0514	0.0515	0.0509	0.0532	0.0532	0.0519	0.0526 \pm 0.0013*			
B (control)	0.0560	0.0511	0.0519	0.0504	0.0508	0.0507	0.0536	0.0528	0.0551	0.0525 \pm 0.0020*			
C	0.1410	0.1543	0.1342	0.1428	0.1429	0.1397	0.1397	0.1399	0.1306	0.1406 \pm 0.0065*	+		+
D	0.1821	0.1881	0.1712	0.1654	0.1566	0.1694	0.1564	0.1568	0.1695	0.1684 \pm 0.0113*	+		+
E	0.5514	0.5017	0.4982	0.5439	0.4578	0.5834	0.4290	0.4423	0.5021	0.5011 \pm 0.0521*	++		+
F	0.3410	0.3325	0.3869	0.3478	0.4421	0.4019	0.3908	0.4063	0.3566	0.3784 \pm 0.0363*	+		+

Note: CHO cells were cultured in DMEM medium supplemented with 10% fetal bovine serum. cDNAs encoding human LGC fusion were cloned into pUHD-30F and were introduced into the CHO cells using Transfast™ according to the manufacturer’s instructions. Two days after transfection, the cells were transferred to selection medium containing 0.722 M (500 mg/ml) G418. After 3 weeks of selection, LGC expression was detected and assessed by ELISA, Western blot, and Fluorescence (and RT-PCR) using anti-beta-amyloid antibody, respectively. The cells were then sorted by fluorescence-activated cell sorting to obtain cell lines expressing high levels of LGC fusion.

^a The ELISA result of expressed proteins in CHO with rabbit anti-beta-amyloid as the first antibody by accounting fluorescence (A_{450}) of the transfected CHO cells; * $P < 0.001$.
^b Using western blot detecting the fluorescence (A_{450}) of the transfected CHO cells with rabbit anti-beta-amyloid antibody.
^c Using microplate reader detecting the fluorescence (OD_{488}) of the transfected CHO cells with EGFP.

Table 1. The detected result of expressed proteins in CHO cells

2.3.4 Western blot using anti-beta-amyloid

The positive cells were detected by Western blotting using rabbit anti-beta-amyloid as the first antibody and HRP-labeling goat anti-rabbit IgG as the secondary antibody. Confluent cultures of CHO cells grown in 60-mm diameter dishes were rinsed with PBS. Following a brief rinse with PBS, cells were harvested by gentle scraping into 5 ml PBS and centrifuged at 200g. LGC fusion was extracted with 100μl cell lysis buffer for Western containing protease inhibitors cocktail (e.g. PMSF), but without reducing agents, followed by a 5 sec sonication to eliminate DNA viscosity. Protein concentration in extracts was determined using BCA reagent. Equal amounts of LGC were loaded and resolved on 18% SDS polyacrylamide gels. Proteins separated by SDS-PAGE were electrotransferred on PVFD (polyvinylidene fluoride) membranes and probed with anti-beta3 antibodies (1:2000 dilution). Immunoreactivity was detected with a corresponding secondary anti-IgG antibody conjugated with HRP (1:10000 dilution) and with an enhanced chemiluminescent (ECL) substrate (Fig. 3).

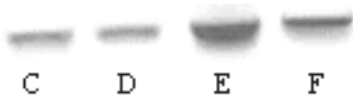


Fig. 3. Western blot results of LGC expressed in CHO cells using anti-amyloid antibody after ELISA results of the transfected CHO cells show positive with anti-amyloid as the first antibody

2.3.5 Fluorescence test

The following detection of LGC fusion stably expressed in CHO cells was determined by fluorescent microscopy. The CHO cells expressing LGC were inoculated in 96-well plate. The fluorescence was read with Tecan Safir microplate reader (excitation at 488 nm wavelength; emission at 507 nm wavelength) at excitation and emission wavelengths of 488 and 507 nm, respectively (table 2). Absorbance value (A_{488}) was used for calculating cell survival rate as follows: survival rate= $(A_{488}$ for experimental group/ A_{488} for control group) $\times 100\%$.

	1	2	3	4	5	6	7	8	Mean \pm S.D.
C	29286	30382	28562	30082	25511	32003	20826	30505	28395 \pm 3599*
D	23461	31222	26847	32466	29306	29002	26725	29544	28572 \pm 2838*
E	30597	32319	29415	33785	30984	30679	30350	27999	30766 \pm 1743*
F	22019	32479	31875	33087	32355	29952	25670	29211	29581 \pm 3899*
control	19996	23069	22992	18006	23385	23408	20639	22474	21746 \pm 1984*

* $P<0.001$ vs group control with the same concentration.

Table 2. The fluorescence values (OD_{488}) of expressed proteins in CHO cells

2.3.6 RT-PCR test

Total RNA was isolated from CHO cells expressing LGC using UNIC-10 trizol total RNA extraction kit. PowerScript reverse transcriptase (Invitrogen) was used to synthesize the first-strand cDNA from an equal amount of the RNA sample. The newly synthesized cDNA templates were further amplified by Platinum *Taq* DNA polymerase (Invitrogen). cDNA sequence of LGC was obtained by the following PCR procedure with plasmid pLGC-30F as template: (1) 95°C for 5 min; (2) 30 cycles at 95°C for 30 sec, 57°C for 60 sec, 72°C for 75 sec; (3) 72°C for 10 min (Yang, et al, 2005; Yang, et al, 2006; Li, et al, 2006). The LGC gene-specific primers 5'-CCTCCGCGGatgctgccggttggcactg-3' and 5'-TCCTCTAGActagttctgcactgctcaaag-3' were used to amplify LGC gene fragment. The samples were restricted with *Sac*II and *Xba*I and further analyzed on 10g/L agarose gel electrophoresis (Fig. 4).

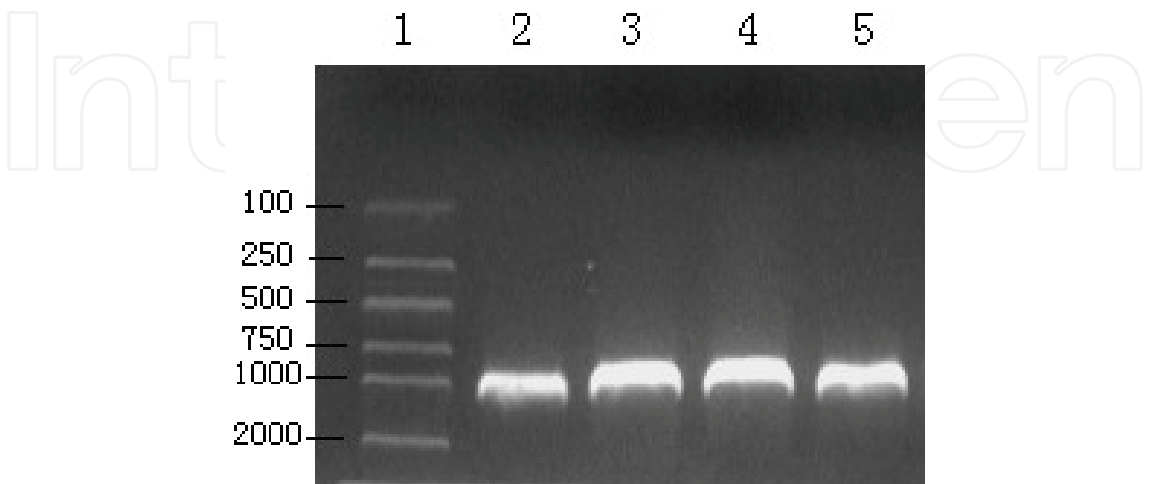


Fig. 4. RT-PCR products on 10g/L agarose gel electrophoresis. Right: 1. DNA marker; DNA marker are 100, 250, 500, 750, 1000 and 2000bp. Left: 2-5. RT-PCR products

2.4 Lithium chloride assay

After CHO cells were transfected with pLGC-30F by CPP method, positive cell colonies were isolated by the selective medium containing geneticin (G418). G418-resistant colonies were limiting dilution in 96 well flat bottomed culture plates at a density of 1.25×10^4 cells per well in the absence of tetracycline to induce expression. Stocks of lithium chloride (LiCl) were prepared in sterile water, whereas compounds were prepared in dimethylsulphoxide. LiCl were added to cells in fresh medium at the final concentrations 0.25 and 0.5 mM, respectively, and media and cells were collected 48 h later. Abeta determinations from media were made by fluorescence assay and ELISA. The fluorescence intensity of CHO cells expressing LGC fusion with EGFP was detected using the microplate reader at an excitation and emission wavelength of 488 nm and 507 nm, respectively. Optical density (OD) determined by ultraviolet spectrophotometry was detected with an ELISA microplate reader at test wavelength of 450nm (table 3).

mM	The fluorescence values (OD ₄₈₈) by EGFP											Mean±S.D.
0.00	41169	43903	42605	41551	44615	46157	45805	48343	42045	42422	43622	43840±2220*
0.25	39132	38565	40417	39567	42697	39193	40993	40909	43352	39795	42658	40662±1626*
0.50	27879	28683	30744	29829	31154	29915	30797	29832	29722	29626	29208	29763±951*
	OD ₄₅₀ by ELISA											
0.00	0.2681	0.2384	0.2354	0.2337	0.2272	0.2348	0.231	0.244	0.2571	0.2375	0.2333	0.2400±0.00015*
0.25	0.1731	0.1613	0.1427	0.151	0.1263	0.1122	0.1196	0.1092	0.1341	0.1315	0.1171	0.1344±0.00043*
0.50	0.1309	0.1384	0.1092	0.112	0.0966	0.0761	0.0946	0.1213	0.1254	0.1315	0.1310	0.1152±0.00038*

* P<0.001 vs group control with the same concentration.

Table 3. Test of the CHO cell model expressing LGC fusion by LiCl

	C (M)	OD570					Inhibiting rate (%)
		1	2	3	4	Mean±S.D.	
Pepstatin A	8.00×10^{-4}	0.48	0.4959	0.4504	0.4876	0.4785±0.0198*	>100
	5.36×10^{-4}	0.3777	0.3765	0.3312	0.3425	0.3570±0.0237*	>100
	2.64×10^{-4}	0.2293	0.2315	0.2498	0.2477	0.2396±0.0107*	>100
	8.00×10^{-5}	0.2011	0.2086	0.202	0.2086	0.2051±0.0041*	90.63
	5.36×10^{-5}	0.175	0.1711	0.1765	0.1651	0.1719±0.0051*	59.82
	2.64×10^{-5}	0.1457	0.1413	0.1469	0.1564	0.1476±0.0064*	37.18
	8.00×10^{-6}	0.1386	0.1357	0.1398	0.1317	0.1365±0.0036*	26.84
Control	0	0.1119	0.1079	0.1007	0.1098	0.1076±0.0049*	

* P<0.001 vs group control with the same concentration.

Table 4. Activity of Pepstatin A by MTT assay

2.5 MTT assay

2.5.1 Activity of pepstatin A

Pepstatin A was aspartic proteinase inhibitor (PDB filecode 2RMP) (Yang & Quail, 1999) as well as beta-secretase inhibitor with IC₅₀ value of 50 mM (Michelle, et al, 2001), which was reported to block solubilized gamma-secretase activity with IC₅₀ value of 4.0 and 5.9 μM, respectively (Li et al, 2000; Zhang et al, 2001).

Tet-CHO cells were incubated in 96 well plates at a density of 2.0×10^4 cells per well overnight. Pepstatin A was prepared in dimethylsulphoxide (DMSO). Pepstatin A was added to cells in fresh medium in the presence of 1 $\mu\text{g/ml}$ Tet (Gossen and Bujard, 1992; Liang et al, 2004) at the final concentrations 8.0×10^{-4} , 5.36×10^{-4} , 2.64×10^{-4} , 8.0×10^{-5} , 5.36×10^{-5} , 2.64×10^{-5} , and 8.0×10^{-6} M, respectively (table 4). 5mg/ml MTT at 20 μl per well were added to the pepstatin-treated or -untreated cells 48 h later. After 4 h, DMSO was added to dissolve the formed formazan crystals. Absorbance of the final product was examined by measuring the optical density at 570 nm using the microplate reader. Absorbance value was used for calculating cell survival rate as follows: survival rate = $(A_{570} \text{ for experimental group} / A_{570} \text{ for control group}) \times 100\%$.

2.5.2 Screening of some compounds

Some compounds (II-16 and II1-II6) under test were prepared in DMSO. Similarly, Tet-CHO cells were incubated into 96-well plates and cultured in DMEM supplemented with 10% FBS. These compounds were added to Tet-CHO cells in fresh medium in the presence of 1 $\mu\text{g/ml}$ Tet at different final concentrations (table 5). After incubation at 37 °C in a 5% CO₂ atmosphere for 48 h, Abeta determinations from media were made by fluorescence assay. The fluorescence intensity of Tet-CHO cells expressing LGC fusion with EGFP was detected using the microplate reader at an excitation and emission wavelength of 488 nm and 507 nm, respectively.

On the other hand, incubated at 37 °C for 48 h later, MTT was added (final concentration 0.5 $\mu\text{g/ml}$) to the compound-treated or -untreated cells for 4 h, then DMSO was added to dissolve the formed formazan crystals. Optical density (OD) was measured with the microplate reader at test wavelength of 570nm. Absorbance value was used for calculating cell survival rate as follows: survival rate = $(A_{570} \text{ for experimental group} / A_{570} \text{ for control group}) \times 100\%$.

2.5.3 Cytotoxicity

The cytotoxic effect of these compounds on normal CHO cells were tested by MTT assay and the IC₅₀ values were calculated from the dose-response curves (Basani et al., 2001; Yang et al., 2009). CHO were incubated into 96-well plates and cultured in DMEM supplemented with 10% FBS. The compounds (Table 5) were added to CHO cells. After incubation at 37 °C for 48 h, MTT was added (final concentration 0.5 $\mu\text{g/ml}$) to the compound-treated or -untreated cells for 4 h, then DMSO was added to dissolve the formed formazan crystals. Absorbance of the final product was examined by measuring the optical density at 570 nm.

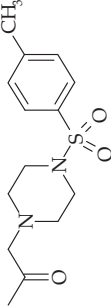
2.6 Statistics

Data are expressed as mean \pm standard deviation (S.D.) throughout this paper. All experiments were performed independently at least thrice. Statistical analyses were performed with Student's *t*-test where significant ($P < 0.01$) differences were found between mean values.

3. Results

3.1 Plasmid pLGC

The consecutive cleavage of APP by beta- and gamma-secretase constitutes the amyloidogenic pathway as it generates Abeta, which plays a critical role in the pathogenesis

No	Structure	Anti-beta-amyloid aggregation		Cell toxicity (CHO)	
		MTT (IC ₅₀ , mM) ^a	Fluorescence ^b	IC ₅₀ (mM) ^c	
Type I	I-1	C ₆ H ₅ SO ₂ -	+	7.71±0.87	
	I-2	p-CH ₃ -C ₆ H ₄ SO ₂ -	+	8.65±1.04	
	I-3	o-NO ₂ -C ₆ H ₄ CO-	+	5.39±0.55	
	I-4	m-NO ₂ -C ₆ H ₄ CO-	+	6.22±0.38	
	I-5	p-NO ₂ -C ₆ H ₄ CO-	+	7.54±0.79	
	I-6 ^[24]		+	8.81±1.63	
Type II	II-1	C ₆ H ₅ CH ₂ -	+	8.86±1.33	
	II-2	m-Cl-C ₆ H ₄ CO-	+	9.11±1.18	
	II-3 ^[42]	m-Br-C ₆ H ₄ CO-	+	8.42±0.77	
	II-4	o-Cl-C ₆ H ₄ CO-	+	6.69±0.86	
	II-5	p-Cl-C ₆ H ₄ CO-	+	5.79±0.57	
	II-6	C ₆ H ₅ SO ₂ -	+	8.67±1.05	

^a The inhibitory concentrations (IC₅₀) of these compounds for anti-beta-amyloid aggregation were evaluated by MTT assay based on Tet-CHO cells expressing EGFP-tagged C99 (LGC fusion). P<0.01; n=3.

^b Using microplate reader detecting the fluorescence (OD₄₈₈) of the transfected CHO cells with EGFP.

^c The inhibitory concentrations (IC₅₀) of these compounds for cell toxicity were evaluated by MTT method using flow cytometry accounting absorbance (A₅₇₀) of CHO cells and Hela cells. P<0.01; n=5.

Table 5. The biological activities of some compounds

of Alzheimer's disease. C99 is derived from cleavage of APP by the protease beta-secretase at the N-terminus of the Abeta-domain, which is further cleaved within its transmembrane domain by gamma-secretase, leading to the secretion of the Abeta peptide. beta-secretase might generate Abeta peptides by cleavage of APP between position Met671 and Asp672 of APP770 as well as gamma-secretase by cleavage of Val711-Ile712 or Ala713-Thr714 of APP770 (Fig. 1). To construct cell model of gamma-secretase inhibitors, we introduced C99 sequence into the structure of gamma-secretase's substrate (LGC fusion), composed of APP's signal peptide, EGFP and C99. The resultant 1.1kb LGC fragment was ligated to replace the *NheI*-*HindIII* restriction fragment of pEGFP-C1 to form pLGC-EGFP. In addition, to utilize the tetracycline-responsive system to express EGFP-tagged C99, the resultant 1.1kb fragment was ligated to replace the *SacII*-*XbaI* fragment of pUHD30F to create pLGC-30F. The expression vectors were transformed into *E. coli* DHalpha5 and confirmed by sequencing analysis (Fig. 2).

3.2 Stable expression of LGC in CHO cells

Tetracycline-inducible expression system includes pUHD30F (vacancy vector for expressing target gene) and p15-1neo (expressing tTA). CHO cells were cultured in DMEM medium supplemented with 10% FBS. pLGC-30F mentioned above in combination with 2 µg of p15-1neo was introduced into the CHO cells via CPP method (Zhu et al, 1997; Zhu, 1999). Cells were subsequently cultured in presence of G418 (1 mg/ml) for 3 weeks and then were detected and assessed by ELISA, fluorescence assay and western blot using anti-beta-amyloid antibody (Table 1). Tetracycline (1 µg/ml) was always included in the culture medium until expression of exogenous LGC fusion was required. G418-resistant colonies, Tet-CHO, were then cultured as a whole in DMEM containing 0.2 mg/ml of G418 and 1 mg/ml of tetracycline.

The ELISA was used to validate LGC expression in transfected cell colonies. The A_{450} of the negative control proteins from 9 CHO cells was 0.0526 ± 0.0013 (mean \pm S.D.). The total range of the A_{450} was 0.1406 to 0.5011 (Table 1). The t test reveals that four samples (C-F clones) are positive, whose A_{450} values were significantly higher than the negative serum sample ($P < 0.001$).

The positive cells were chosen for the identification of LGC by Western blotting using mouse anti-beta-amyloid as the first antibody and HRP-conjugated goat anti-rabbit IgG as the second antibody (Fig. 3). Comparison of the assay results between ELISA and western blot displayed that three samples (C, D, E and F clones) are positive; the protein expression amount of E is higher than that of C, D and F, which is supported by fluorescence assay (Table 2) and RT-PCR analyses (Fig. 4).

LiCl were added to Tet-CHO cells in fresh medium at different concentrations. After 48 h, Abeta determinations from media were made by fluorescence assay (A_{488}) and ELISA (A_{450}) (Table 3). The A_{488} and A_{450} of the negative control were 43840 ± 2220 and 0.2400 ± 0.00015 , respectively. The t test shows that LiCl at a concentration of 0.25 and 0.5 nM are positive, whose A_{450} values were significantly higher than the control sample ($P < 0.001$).

The extent of inhibiting Abeta generation and assembly of pepstatin A was measured by MTT assay. Inhibiting rate of different concentrations of pepstatin A are >100%, 90.63%, 58.82%, 37.18% and 26.84%, respectively, whose IC_{50} (half-maximal inhibitory concentration) values is approximately 35.83 µM (Table 4), which is consist with the research results (pepstatin A with IC_{50} value of 35 µM) of Campbell's group (Campbell et al, 2002). This also

verified that Tet-CHO cell model can be used for detection of gamma-secretase inhibitor activity.

3.3 Activity of some new compounds

To determine their molecular basis, the ability of these compounds to inhibit EGFP-tagged C99 binding to gamma-secreasase were measured based on the Tet-CHO cells. Fluorescence assay reveals that these compounds inhibited production of Abeta by interfering gamma-secreasase. Similarly, the IC_{50} values for inhibiting Abeta generation and assembly of compounds **I1-I6** and **II1-II6** were 0.819 to 81.920 mM (Table 5), while IC_{50} of pepstatin A is 35.83 μ M, which is consistent with Campbell's results (pepstatin A with IC_{50} value of 35 μ M) (Campbell et al, 2002).

Cytotoxicity profiles of compounds **I1-I6** and **II1-II6** treated on Tet-CHO cells were compared with the standard CHO cell-based MTT assay. Their cytotoxicity assay on Tet-CHO cells was more sensitive than that on the standard CHO cells, and nine compounds **I1, I2, I3, I4, II1, II2, II4, II5** and **II6** with IC_{50} values of 5.39 to 9.91 mM (Table 5). Especially, compounds **I1, I3, II1, II4**, and **II6** show higher anti- Abeta activities with a sort order of **I1 > II4 > II6 > II1 > I3**. Further evaluation is under investigation.

Comparison of their anti-Abeta activities with their cytotoxicities displayed that nine compounds **I1, I2, I3, I4, II1, II2, II4, II5** and **II6** are positive, especially compounds **I1, I3, II1, II4**, and **II6** show higher anti-Abeta activities but lower than pepstatin A.

4. Discussion

A system for tetracycline-regulated inducible gene expression has been described which relies on constitutive expression of a tetracycline-controlled transactivator (tTA) fusion protein combining the tetracycline (Tet) repressor (tetR) and the transcriptional activation domain of virion protein 16 (VP16). In the Tet-Off expression system, *tTA* regulates expression of a target gene that is under transcriptional control of a tetracycline-responsive promoter element (TRE), which is made up of Tet operator (tetO) sequence concatemers fused to the human cytomegalovirus (hCMV) immediate-early promoter (Gossen, & Bujard, 1992). The specificity of the Tet repressor-operator-effector interaction and the pharmacological characteristics of Tet's make this autoregulatory system well suited for the control of gene activities both in cultured cells and in transgenic animals (Gossen, et al, 1995; Shockett, et al, 1995). For example, Zhu's group has researched regulation of cell motilities by expression of nuclear distributions (Nud) (Yan et al, 2003; Liang et al, 2004; Liang et al, 2007; Ma et al, 2009), mitotin (Zhu, 1999; Zhou et al, 2005; Yang et al, 2003), etc. (Shen et al, 2008; Shan et al, 2009; Ding et al, 2009; Zhang et al, 2009), under the control of tetracycline-inducible Tet-off system.

Additionally, the green fluorescent protein (GFP) from the jellyfish *Aequorea victoria* has become a useful tool in molecular and cell biology, as its intrinsic fluorescence can be visualized in living cells (Elsiger, et al., 1999), especially the enhanced green fluorescent protein (EGFP) widely used as a molecular tag in cell biology (Pan, et al., 2009). GFP emits a bright green light when expressed in either eukaryotic or prokaryotic cells and illuminated by blue or UV light. GFP has generated intense interest as a marker for gene expression and localization of gene products (Ormoe, et al., 1996). The crystal structure of recombinant wild-type GFP reveals also that the protein is in the shape of a cylinder, comprising 11

strands of beta-sheet with an alpha-helix inside and short helical segments on the ends of the cylinder. The fluorophore (chromophore), resulting from the spontaneous cyclization and oxidation of the sequence -Ser65 (or Thr65)-Tyr66-Gly67-, are protected inside the cylinders and requires the native protein fold for both formation and fluorescence emission (Ormoe, et al., 1996; Yang, et al., 1996). Up to now, the numerous applications include: using GFP as a reporter for gene expression, as a marker to study cell lineage during development and as a tag to localize proteins in living cells (Gerdes & Kaether, 1996). Here we focus on the use of EGFP as a protein tag and upon those applications of this new tool in which EGFP promises to be truly superior to conventional methods.

This experiment is to design a drug screening cell model for gamma-secretase inhibitors. So far, the specific components of gamma-secretase, composed of PS, APL-1, PEN-2 and nicastrin, and its mechanism have not yet established. In view of the wide distribution of gamma-secretase in a variety of cell lines and tissues, as well as testing of new beta-secretory inhibitors or gamma-secretase inhibitors using APP transgenic cell or APP transgenic animal, we utilized the tetracycline-responsive system to express EGFP-tagged C99 fusion as a gamma-secretase substrate in the cultured CHO cells and validated by ELISA and Western blot for the following evaluation of the efficiency of some compounds.

To further construct cell model for screening gamma-secretase inhibitors, we designed a novel fusion as gamma-secretase's substrate based on the structural basis of the proteolytical cleavages of APP. C99 was further defined as the domain of APP for gamma-secretase's substrate due to APP processing pathways and Aβ production, resulting from sequential cleavage of APP by proteases named beta- and gamma-secretases (Walsh, et al., 2007; Mouradian, 2007; Roßner et al, 2006). BACE1 (beta-secretase) might generate Aβ peptides by cleavage of APP between position Met671 and Asp672 of APP770 as well as gamma-secretase by cleavage of Val711-Ile712 or Ala713-Thr714 of APP770 (Fig. 1). Elevated Aβ42 levels, as well as particularly the elevation of the ratio of Aβ42 to Aβ40, has been identified as important in early events in the pathogenesis of AD (Mouradian, 2007). Here, C99 sequence was introduced into the structure of gamma-secretase's substrate (LGC fusion). The region coding for EGFP was from pEGFP-C1, added to the structure of gamma-secretase's substrate. To link EGFP to C99, BspE I restriction site was introduced into 3' reverse primer of EGFP and 5' forward primer of C99, respectively. To render membrane localization of LGC fusion, a sequence coding for APP's signal peptide was introduced by the 5' forward synthesized primers in frame into the *NheI* site located before the EGFP-coding sequence and C99 cDNA. The resultant 1.1kb fragment was ligated to replace the *NheI*-*HindIII* restriction fragment of pEGFP-C1 (nucleotides 592 to 1352) to form pLGC-EGFP (Fig. 2). pLGC-EGFP was constructed from pEGFP-C1 to express LGC fusion with a signal peptide at N termini as in APP. To utilize the tetracycline-responsive system (Zhu, 1999) to express EGFP-tagged C99, the resultant 1.1kb fragment was ligated to replace the *SacII*-*XbaI* fragment of pUHD30F to create pLGC-30F. The expression vectors (pLGC-EGFP and pLGC-30F) were transformed into *Escherichia coli* DHα5 in order to verify the correct sequence through sequence analysis (Fig. 2). It is necessary to connect EGFP gene to the N-terminal of the gamma-secretase substrate C99 in order to facilitate screening. Only the pair of plasmids were stably transfected into CHO cells, target gene was able to expressed and the cells show fluorescent. EGFP fluoresces under certain wavelengths of ultraviolet excitation can be easily detected, but also its molecular weight is relatively small so that the basic structures of the proteins fused with EGFP do not been affected and the proteins can play their normal function.

In a previous study, our group has constructed the drug screening cell model applied to some compounds inhibiting FITC-fibrinogen binding to human α IIb β 3 expressed in CHO cells (Yang et al, 2009). We utilized the tetracycline-responsive system (Zhu, 1999) to express EGFP-tagged C99 fusion as a gamma-secretase substrate. Expression levels were indeed reduced under control of either the cytomegalovirus promoter or the tetracycline-responsive promoter. p15-1 neo included is essential for activation of the tetracycline-responsive promoter in the pUHD30F vector. Moreover, the tetracycline inducible system (pUHD30F and p15-1 neo) contains switching mechanism, and close the expression of substrate (pUHD30F-C99) by adding Tet (or Dox) in Tet-off system to avoid generation of Abeta and its cell toxicity. The dual-plasmid system of the Tet-off system transfected CHO cells to build a cell model for anti-Abeta drug screen. G418-resistant cell lines were screened for conditional expression of LGC and the stable expression cell lines (Tet-CHO) was obtained. Cell lines transfected with just the expression vector were isolated as controls. Clones displaying highly regulated expression were obtained for LGC. It should be noted, however, that all clones exhibited a low basal level of LGC expression in the presence of tetracycline, which was detectable in most of the experiments performed. Then, added positive drugs (LiCl and pepstatin A) to validate whether this cell model has the effect of function for detection of gamma-secretase inhibitors. Finally, the cell model was capable of screening other compounds for discovery of new gamma-secretase inhibitors.

Glycogen synthase kinase 3 (GSK3) is a constitutively active, proline-directed serine/threonine kinase that plays a part in a number of physiological processes ranging from glycogen metabolism to gene transcription. GSK3 also plays a pivotal and central role in the pathogenesis of both sporadic and familial forms of AD. The over-activity of GSK3 accounts for memory impairment, tau hyper-phosphorylation, increased beta-amyloid production and local plaque-associated microglial-mediated inflammatory responses; all of which are hallmark characteristics of AD. The inhibitors of GSK3 would provide a novel avenue for therapeutic intervention in this devastating disorder (Hooper, et al., 2008). Inhibition of GSK3 by LiCl has been reported to reduce Abeta (Phiel, et al., 2003; Sun, et al., 2002), perhaps through presenilin-dependent gamma-secretase inhibition (Netzer, et al., 2003). Abeta peptides are derived from APP by sequential proteolysis, catalysed by beta-secretase, followed by presenilin-dependent gamma-secretase cleavage (Phiel, et al., 2003). Besides interaction with nicastrin, APH-1 and PEN-2 required for gamma-secretase function, presenilins also interact with alpha-catenin, beta-catenin and GSK-3 (Francis et al, 2002). The therapeutic concentrations of LiCl, a GSK3 inhibitor, block the production of Abeta peptides by interfering with APP cleavage at the gamma-secretase step, but do not inhibit Notch processing. Importantly, lithium also blocks the accumulation of Abeta peptides in the brains of mice that overproduce APP. The target of lithium in this setting is GSK-3, which is required for maximal processing of APP. Since GSK-3 also phosphorylates tau protein, the principal component of NFTs, inhibition of GSK-3 offers a new approach to reduce the formation of both amyloid plaques and NFTs, two pathological hallmarks of AD (Phiel, et al., 2003). Here, we added LiCl to Tet-CHO cells expressing EGFP-tagged C99 fusion. The results of ELISA and fluorescence assay revealed that LiCl inhibited the production of Abeta at a concentration of 0.25 and 0.5 mM with the inhibiting rates of 7.25% and 32.11% by fluorescence assay, respectively (or 44% and 52% by ELISA, respectively) (Table 3), which is supported by the research results of Phiel's group (LiCl with an IC_{50} of 1–2mM) (Phiel, et al., 2003), and consistent with a report using transient overexpression of the APP carboxy terminus C100 in COS7 cells (Sun, et al., 2002).

Pepstatin A was aspartic proteinase inhibitor (PDB filecode 2RMP) (Yang & Quail, 1999) as well as beta-secretase inhibitor with IC_{50} value of 50 mM (Michelle, et al, 2001), which was reported to block solubilized gamma-secretase activity (Li et al, 2000). When C100Flag was used as a gamma-secretase substrate in an in vitro assay, the IC_{50} for pepstatin A to inhibit Abeta40 and Abeta42 generation was 4.0 and 5.9 μ M, respectively (Li et al, 2000). A cell-free assay on membrane vesicles derived from C99-transfected cells showed that the IC_{50} of pepstatin A for inhibition of both Abeta40 and Abeta42 was estimated at $\sim 4\mu$ M (Zhang et al, 2001). Because both C100Flag and C99 are immediate substrates for gamma-secretase, it is not surprising to see an IC_{50} for pepstatin A at 35 μ M when Campbell and co-worker used microsomes derived from full length (FL) APP expressing cells (Campbell et al, 2002). Here, we built Tet-CHO cells expressing EGFP-tagged C99 fusion (LGC) with 17-residue signal peptide of APP and obtained an IC_{50} for pepstatin A at 35.83 μ M employing MTT assay, similar to Campbell's method. And Campbell et al have found that pepstatin A was shown to bind to PS1 with higher affinity to FL PS1 than to PS1 fragments. The high efficacy of pepstatin A binding to FL PS1 may lead to efficient inhibition of endoproteolysis compared to the low efficacy of binding to functional NTF/CTF complexes and inhibition of gamma-secretase cleavage in the Golgi/TGN (Campbell et al, 2002).

Fluorescence and MTT assay revealed that twelve new 2-substituted-1,2,3,4-tetrahydroisoquinoline derivatives (**I-1-I-6** and **II-1-II-6**) inhibited production and assemblage of Abeta to some extent by interfering gamma-secrease (Table 5). Especially, compounds **I-1**, **I-3**, **II-1**, **II-4**, and **II-6** showed higher anti-Abeta activities while their cytotoxicity assay on Tet-CHO cells was more sensitive than that on the standard CHO cells. However, their IC_{50} values (from 0.819 to 81.920 mM) for inhibiting Abeta assembly (Table 5) were smaller than that of pepstatin A. Our results displayed that their anti-Abeta activities depended on the substitutes at position 2 of the tetrahydroisoquinoline nucleus. Phenylsulfonyl, benzyl or ortho-substituted benzoyl derivatives have higher anti-Abeta activities, such as compounds **I-1**, **I-3**, **II-1**, **II-4**, and **II-6**, which is supported by our previous research results that the phenylsulfonyl group is necessary (Yang et al., 2009). Electron-withdrawing groups (EWG) at the position ortho of benzene are propitious to anti-Abeta activities, such as chlorine (**II-4**) and nitril groups (**I-3**). Similarly, electron-donating groups (WDG) at the position para of phenylsulfonyl group are not beneficial to their anti-Abeta activities, such as compound **I-2**. The anti-Abeta activities of unsubstituted phenylsulfonyl derivatives (**I-1** and **II-6**) are evidently higher than that of **I-2**. We have reported that the nitrogen atom at 2 position of 1,2,3,4-tetrahydroisoquinoline interacted with the carboxyl group at the side chain of Asp179 of integrin alpha2b in the fashion of electrostatic interaction (Yang et al, 2009). Here the sulphonyl and carbonyl group at 2 position of 1,2,3,4-tetrahydroisoquinoline may interact with gamma-secrease in the same fashion to exhibit anti-Abeta activities. On the other hand, our previous research has also exhibited that compound **I-6** possessed higher anti-platelet aggregation by inhibiting fibrinogen binding to its receptor GPIIbIIIa (integrin alpha2bbeta3) with IC_{50} value of approximately 37.13 μ M (Yang et al, 2009). Molecular modeling indicated that this compound might interact with fibrinogen receptor by Thr125 residue of beta3, Tyr166 and Asp179 residues of alpha2b, especially the hydroxyl groups of Thr125 and Tyr166 and the carboxyl group at side chain of Asp179. Interestingly, the anti-platelet aggregation activities of type II compounds have ever reported as well as ticlopidine (Yang et al, 2004). Their antiplatelet aggregatory activity is related to the sizes of substitutes, as well as charge or

electronegativity, which is consistent with the CoMFA study results: the steric and electrostatic interactive energy is the major contribution to antiplatelet aggregatory activity, and an area accommodating a small weak-polar group exists near the 7 position of the tetrahydroisoquinoline nucleus.

Interestingly, these compounds possessed anti-Abeta activities as well as anti-platelet aggregation activities, and they may play important roles in AD therapy by fibrin-guided signal pathway (Adams, et al, 2004). Merkle and co-worker have indicated that vascular deposition of Abeta is associated with recurrent intracerebral hemorrhages in certain disease states and revealed a network of fibrin (Fn) and amyloid fibers formed in the presence of Abeta with significantly decreased lateral Fn-Fn interactions using electron microscopic analysis, namely Abeta significantly altering the nature of the Fn obtained in its presence (Merkle et al, 1996). Since platelets are the principal source of both APP and Abeta in human blood, AD platelet activation may reflect or even contribute to the pathogenesis of the disease (Sevush et al, 1998). These results suggest that fibrin is a mediator of inflammation and may impede the reparative process for neurovascular damage in AD. Fibrin and the mechanisms involved in its accumulation and clearance may present novel therapeutic targets in slowing the progression of AD (Paul et al, 2007). Fibrin receptors are defined as membrane-bound proteins that can transduce intracellular signals upon fibrin binding, whereas fibrin binding proteins are either soluble or anchored molecules that bind fibrin but have no documented ability to directly transduce intracellular signals upon fibrin binding. The functional consequences of these protein-fibrin interactions range from blood coagulation and initiation of angiogenesis, to inflammation and propagation of infection (Adams, et al, 2004). Fibrin binds several families of integrins, including beta₁, beta₂, and beta₃ subtypes. Fibrin-integrin interactions mediate a variety of cellular responses, including clotting and inflammation via the mitogen-activated protein kinase (MAPK), the phosphoinositide-3 kinase (PI3K), or the NF-κB signal pathways. Moreover, reducing fibrinogen, a circulating protein critical in hemostasis, provides a significant decrease in the neurovascular damage, blood-brain barrier permeability and neuroinflammation present in AD. These studies implicate fibrinogen as a possible contributor to AD (Cortes-Canteli & Strickland, 2009). In addition, platelet-derived growth factor (PDGFs) has been indicated that it can induce the beta-gamma-secretase-mediated cleavage of APP through a Src-Rac-dependent pathway (Gianni et al, 2003). Studies of PDGFs and their receptors have revealed roles for PDGF signaling in gastrulation and in the development of the cranial and cardiac neural crest, gonads, lung, intestine, skin, CNS, and skeleton as well as blood vessel formation and early hematopoiesis (Andrae et al, 2008). PDGF signaling is implicated in a range of diseases, such as certain gliomas, sarcomas, leukemias, epithelial cancers, vascular disorders, and fibrotic diseases, involving tumor growth, angiogenesis, invasion, and metastasis. How these compounds to inhibit both platelet aggregation and Abeta accumulation and its mechanism are under investigation.

5. Conclusion

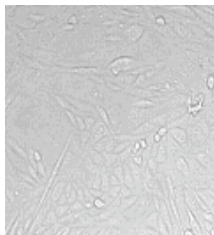
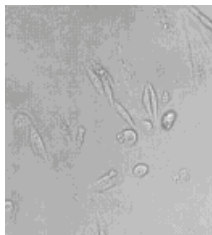
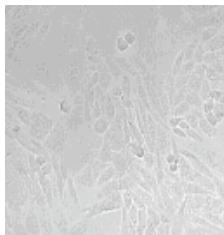

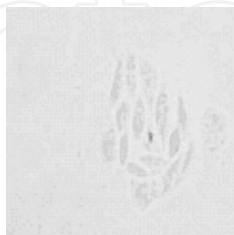
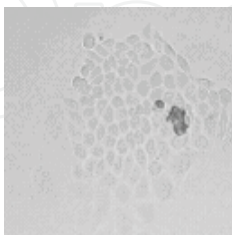
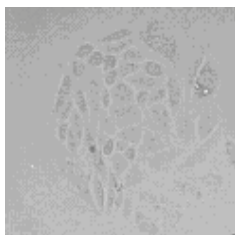
This experiment is to design a drug screening cell model (Tet-CHO) for gamma-secretase inhibitors. In view of the specific components of gamma-secretase, we utilized the tetracycline-inducible Tet-off system to express EGFP-tagged C99 fusion as a gamma-secretase substrate in the cultured CHO cells and validated by ELISA and Western blot for the following evaluation of the efficiency of some compounds. Additionally, twelve

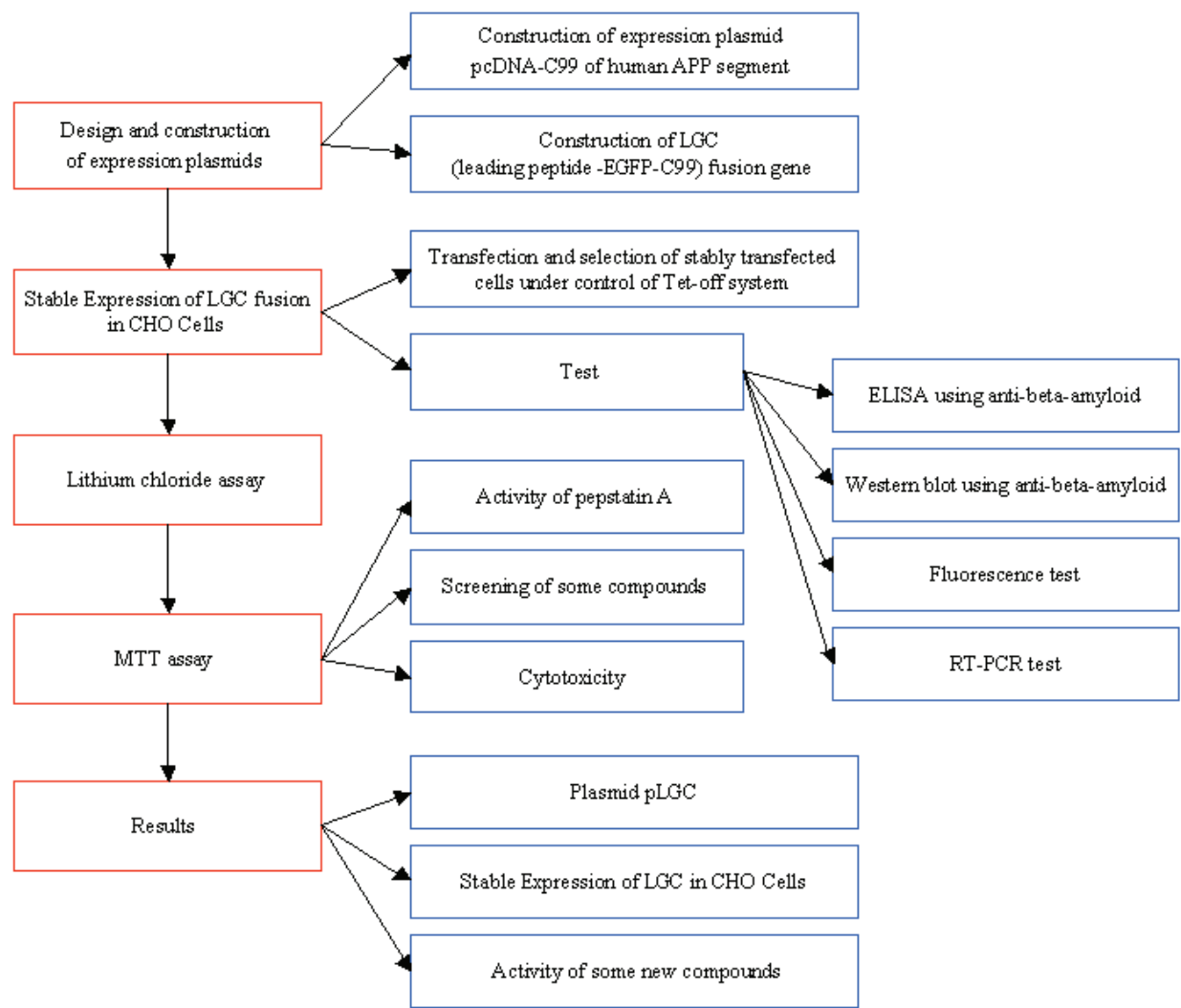
2-substituted 1,2,3,4-tetrahydroisoquinoline derivatives were designed and synthesized by the aid of computer drug design, based on the principles of isosterism and the reported SAR of synthesized tetrahydroisoquinoline derivatives. These compounds have anti-Abeta accumulation activity by inhibiting gamma-secretase interaction with its substrate, EGFP-tagged C99. The phenylsulfonyl derivatives (compound **I-1** and **II-6**), the benzyl derivative **II-1**, and the benzoyl derivatives (**I-3** and **II-4**) showed higher anti-Abeta activities, which is supported by our previous research results that the phenylsulfonyl group is necessary (Yang et al., 2009). Especially compound **I-6** has not only anti-Abeta accumulation activity but also anti-platelet aggregation activity, suggesting a potential role of fibrin-guided signal pathway in AD therapy.

6. Acknowledgments

This work is supported by Nature Science Fund of China (No. 30171094 and No. 30271497).

Appendix 1. The growth properties of G418-resistant cells during three weeks

time	Annotation time		Annotation		
2 days		Some cells begin to age and cell rounding.	8 days		The drug-resistant cell lines survive.
5 days		Cells begin to die.	12 days		Single cells began to amplification
15 days		cells amplification and colony-forming unit	21 days		Form a stable clone.
18 days		Colony-forming unit			



Flowchart for construction of drug screening cell model and its application

7. References

Adams, R. A.; Passino, M.; Sachs, B.D.; Nuriel, T. & Akassoglou, K. (2004). Fibrin Mechanisms and Functions in Nervous System Pathology. *Mol. Interv.*, Vol. 4, No. 3, (Jun 2004), pp163-176, ISSN 1534-0384.

Andrae, J.; Gallini, R. & Betsholtz C. (2008). Role of platelet-derived growth factors in physiology and medicine. *Genes Dev.*, Vol. 22, No. 10, (May 2008), pp1276-1312, ISSN 0890-9369.

Baron, U.; Gossen, M. & Hermann Bujard, H. (1997). Tetracycline-controlled transcription in eukaryotes: novel transactivators with graded transactivation Potential. *Nucleic Acids Research*, Vol. 25, No. 14, (Jul 1997), pp 2723-2729, ISSN 0305-1048.

Campbell, W.A.; Iskandar, M.-K.; Reed, M.L.O. & Xia, W. (2002). Endoproteolysis of Presenilin in Vitro: Inhibition by gamma-Secretase Inhibitors. *Biochemistry*, Vol. 41, No. 10, (May 2002), pp3372-3379, ISSN 0006-2960.

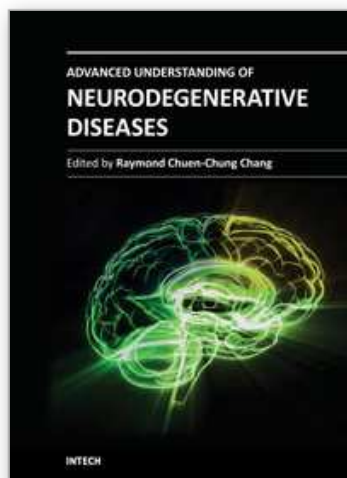
Carter, D.B.; Chou, K.C. (1998). A model for structure dependent binding of Congo Red to Alzheimer beta-amyloid fibrils. *Neurobiol. Aging*, Vol. 19, No. 1, (Jan.-Feb 1998), pp37-40, ISSN 0197-4580.

- Cook, D.G.; Sung, J.C.; Golde, T.E.; Felsenstein, K.M.; Wojczyk, B.S.; Tanzi, R.E.; Trojanowski, J.Q.; Lee, V.M.-Y. & Doms, R.W. (1996). Expression and analysis of presenilin 1 in a human neuronal system: localisation in cell bodies and dendrites. *Proc. Natl. Acad. Sci. U.S.A.*, Vol. 93, No. 17, (Aug 1996), pp9223-9228, ISSN 0027-8424.
- Ding, C.; Liang, X.; Ma, L.; Yuan, X. & Zhu, X. (2009). Opposed effect of Ndel1 and alpha1/2 on cytoplasmic dynein functions through competitive binding to Lis1. *J Cell Sci.*, Vol. 122, No. 16, (Aug 2009), pp 2820-2827, ISSN 0021-9533.
- Elslinger, M.A.; Wachter, R.M.; Hanson, G.T.; Kallio, K. & Remington, S.J. (1999). Structural and spectral response of green fluorescent protein variants to changes in pH. *Biochemistry*, Vol. 38, No. 17, (Apr 1999), pp 5296-5301, ISSN 0006-2960.
- Findeis, M.A. (2007). The role of amyloid beta peptide 42 in Alzheimer's disease. *Pharmacology & Therapeutics*, Vol. 116, No. 2, (Jul 2007), pp 266-286, ISSN 0163-7258.
- Francis, R.; McGrath, G.; Zhang, J.; Ruddy, D.; Sym, M.; Apfeld, J.; Nicoll, M.; Maxwell, M.; Hai, B.; Ellis, M.; Parks, A.L.; Xu, W.; Li, J.; Gurney, M.; Myers, R.L.; Himes, C.S.; Hiebsch, R.; Ruble, C.; Nye, J.S. & Curtis, D. (2002). aph-1 and pen-2 are required for Notch pathway signalling, g-secretase cleavage of bAPP, and presenilin protein accumulation. *Dev. Cell*, Vol. 3, No. 1, (Jul 2002), pp 85-97, ISSN 1534-5807.
- Ge, H.M.; Zhu, C.H.; Shi, D.H.; Zhang, L.D.; Xie, D.Q.; Yang, J.; Ng, S.W. & Tan, R.X. (2008). Hopeahainol A, An Acetylcholinesterase Inhibitor from Hopea hainanensis. *Chem. Eur. J.*, Vol. 14, No. 1, (Jan 2008), pp376-381, ISSN 1521-3765.
- Gerdes, H.-H. & Kaether, C. (1996). Green fluorescent protein: applications in cell biology. *FEBS Lett.*, Vol. 389, No. 1, (Jun 1996), pp 44-47, ISSN 0014-5793.
- Gianni, D.; Zambrano, N.; Bimonte, M.; Minopoli, G.; Mercken, L.; Talamo, F.; Scaloni, A. & Russo, T. (2003). Platelet-derived Growth Factor Induces the beta-gamma-Secretase-mediated Cleavage of Alzheimer's Amyloid Precursor Protein through a Src-Rac-dependent Pathway. *J. Biol. Chem.*, Vol. 278, No. 11, (Mar 2003), pp 9290-9297, ISSN 0021-9258.
- Goo, J.H. & Park, W.J. (2004). Elucidation of the Interactions between C99, Presenilin, and Nicastrin by the Split-Ubiquitin Assay. *DNA Cell Biol.*, Vol. 23, No. 1, (Jan 2004), pp 59-65, ISSN 1044-5498.
- Gossen M, Bujard H. Tight control of gene expression in mammalian cells by tetracycline-responsive promoters. *Proc Natl Acad Sci U S A.*, Vol. 89, No. 12, (Jun 1992), pp 5547-5551, ISSN 0027-8424.
- Gossen, M.; Freundlieb, S.; Bender, G.; Muller, G.; Hillen, W. & Bujard, H. (1995). Transcriptional activation by tetracyclines in mammalian cells. *Science*, Vol. 268, No. 5218, (Jun 1995), pp 1766-1769, ISSN 0036-8075.
- Hardy, J. (1997). Amyloid, the presenilins and Alzheimer's disease. *Trends Neurosci.*, Vol. 20, No. 4, (Apr 1997), pp 154-159, ISSN 0166-2236.
- Hartmann, T.; Bieger, S.C.; Bruhl, B.; Tienari, P.J.; Ida, N.; Allsop, D.; Roberts, G.W.; Masters, C.L.; Dotti, C.G.; Unsicker, K. & Beyreuther, K. (1998). Distinct sites of intracellular production for Alzheimer's Ab40/42 amyloid peptides. *Nature Med.*, Vol. 3, No. 9, (Sep 1998), pp 1016-1020, ISSN 1078-8956.
- Hooper, C.; Killick, R. & Lovestone, S. (2008). The GSK3 hypothesis of Alzheimer's disease. *J Neurochem.*, Vol. 104, No. 6, (Mar 2008), pp 1433-1439, ISSN 0022-3042.
- Jiang, X.F.; Yang, J. & Wang, W. (2006). The Complex Network of Protein-Protein Interaction of Alzheimer's Disease Associated Proteins and an Interaction Predicting. *Journal of Nanjing University (Natural Science)*, Vol. 42, No. 5, (May 2006), pp 479-489, ISSN 0469-5097.

- Kaether, C.; Haass, C. & Steiner, H. (2006). Assembly, trafficking and function of gamma-secretase. *Neurodegener Dis.*, Vol. 3, No. 4-5, (Oct 2006), pp 275-283, ISSN 1660-2854.
- Kelliher, M.; Fastbom, J.; Cowburn, R.F.; Bonkale, W.; Ohm, T.G.; Ravid, R.; Sorrentino, V. & O'Neill, C. (1999). Alterations in the ryanodine receptor calcium release channel correlate with Alzheimer's disease neurofibrillary and beta-amyloid pathologies. *Neuroscience*, Vol. 92, No. 2, (May 1999), pp 499-513, ISSN 0306-4552.
- Kovacs, D.M.; Fausett, H.J.; Page, K.J.; Kim, T.-W.; Moir, R.D.; Merriam, D.E.; Hollister, R.D.; Hallmark, O.G.; Mancini, R.; Felsenstein, K.M.; Hyman, B.T.; Tanzi, R.E. & Wasco, W. (1996). Alzheimer-associated presenilins 1 and 2: neuronal expression in brain and localization to intracellular membranes in mammalian cells. *Nature Med.*, Vol. 2, No. 2, (Feb 1996), 224-229, ISSN 1078-8956.
- Li, Y.M.; Lai, M.T.; Xu, M.; Huang, Q.; DiMuzio-Mower, J.; Sardana, M.K.; Shi, X.P.; Yin, K.C.; Shafer, J.A. & Gardell, S.J. (2000). Presenilin 1 is linked with gamma-secretase activity in the detergent solubilized state. *Proc. Natl. Acad. Sci. U.S.A.*, Vol. 97, No. 11, (May 2000), pp 6138-6143, ISSN 0027-8424.
- Liang, Y.; Yu, W.; Li, Y.; Yang, Z.; Yan, X.; Huang, Q. & Zhu, X. (2004). Nudel functions in membrane traffic mainly through association with Lis1 and cytoplasmic dynein. *J. Cell Biol.*, Vol. 164, No. 4, (Feb 2004), pp 557-566, ISSN 0021-9525.
- Liang, Y.; Yu, W.; Li, Y.; Yu, L.; Zhang, Q.; Wang, F.; Yang, Z.; Du, J.; Huang, Q.; Yao, X. & Zhu, X. (2007). Nudel modulates kinetochore association and function of cytoplasmic dynein in M phase. *Mol. Biol. Cell.*, Vol. 18, No. 7, (Jul 2007), pp 2656-2666, ISSN 0270-7306.
- Cortes-Canteli, M. & Strickland, S. (2009). Fibrinogen, a possible key player in Alzheimer's disease. *J. Thromb. Haemost.*, Vol. 7, Suppl. 1, (Jul 2009), pp 146-150, ISSN 1538-7933.
- Ma, L.; Tsai, M.-Y.; Wang, S.; Lu, B.; Chen, R.; Yates, III JR.; Zhu, X. & Zheng, Y. (2009). Requirement for Nudel and dynein for assembly of the lamin B spindle matrix. *Nat. Cell Biol.*, Vol. 11, No. 3, (Mar 2009), pp 247-256, ISSN 1465-7392.
- McLendon, C.; Xin, T.; Ziani-Cherif, C.; Murphy, M.P.; Findlay, K.A.; Lewis, P.A.; Pinnix, I.; Sambamurti, K.; Wang, R.; Fauq, A. & Golde, T.E. (2000). Cell-free assays for gamma-secretase activity. *FASEB J.*, Vol. 14, No. 15, (Dec 2000), pp 2383-2386, ISSN 0892-6638.
- Merkle, D.L.; Cheng, C.H.; Castellino, F.J. & Chibber, B.A. (1996). Modulation of fibrin assembly and polymerization by the beta-amyloid of Alzheimer's disease. *Blood Coagul Fibrinolysis*, Vol. 7, No. 6, (Sep 1996), pp 650-658, ISSN 0957-5235.
- Michelle, L.S.; Turner, R.S. & James, R.G. (2001). The protease inhibitor, MG132, blocks maturation of the amyloid precursor protein Swedish mutant preventing cleavage by beta-secretase. *J. Biol. Chem.*, Vol. 276, No. 6, (Feb 2001), pp 4476-4484, ISSN 0021-9258.
- Mouradian, M.M. (2007). The role of amyloid beta peptide 42 in Alzheimer's disease. *Pharmacology & Therapeutics*, Vol. 116, No. 2, (Nov 2007), pp 266-286, ISSN 0163-7258.
- Netzer, W.J.; Dou, F.; Cai, D.; Veach, D.; Jean, S.; Li, Y.; Bornmann, W.G.; Clarkson, B.; Xu, H. & Greengard, P. (2003). Gleevec inhibits beta-amyloid production but not Notch cleavage. *Proc. Natl. Acad. Sci. U. S. A.*, Vol. 100, No. 21, (Oct 2003), pp 12444-12449, ISSN 0027-8424.
- Ormoe, M.; Cubitt, A.B.; Kallio, K.; Gross, L.A.; Tsien, R.Y. & Remington S.J. (1996). Crystal structure of the *Aequorea victoria* green fluorescent protein. *Science*, Vol. 273, No. 5, (Nov 1996), pp 1392-1395, ISSN 0036-8075.

- Paul, J.; Strickland, S. & Melchor, J.P. (2007). Fibrin deposition accelerates neurovascular damage and neuroinflammation in mouse models of Alzheimer's disease. *J Exp Med.*, Vol. 204, No. 8, (Aug 2007), pp 1999-2008, ISSN 0022-1007.
- Phiel, C.J.; Wilson, C.A.; Lee, V. M. & Klein, P.S. (2003). GSK-3alpha regulates production of Alzheimer's disease amyloid-beta peptides. *Nature*, Vol. 423, No. 6938, (May 2003), pp 435-439, ISSN 0028-0836.
- Resnitzky, D.; Gossen, M.; Bujard, H. & Reed, S.I. (1994). Acceleration of the G(1)/S phase-transition by expression of Cyclin-D1 and Cyclin-E with an inducible system. *Molecular and Cellular Biology*, Vol. 14, No. 3, (Mar 1994), pp 1669-1679, ISSN 0270-7306.
- Roßner, S.; Sastre, M.; Bourne, K. & Lichtenthaler, S.F. (2006). Transcriptional and translational regulation of BACE1 expression—Implications for Alzheimer's disease. *Progress in Neurobiology*, Vol. 79, No. 2, (Jun 2006), pp 95-111, ISSN 0301-0082.
- Ryoo, H.M.; Hoffmann, H.M.; Beumer, T.; Frenkel, B.; Towler, D.A.; Stein, G.S.; Stein, J.L.; van Wijnen, A.J. & Lian, J.B. (1997). Stage-Specific Expression of Dlx-5 during Osteoblast Differentiation: Involvement in Regulation of Osteocalcin Gene Expression. *Molecular Endocrinology*, Vol. 11, No. 11, (Oct 1997), pp 1681-1694, ISSN 0888-8809.
- Sevush, S.; Jy, W.; Horstman, L.L.; Mao, W.W.; Kolodny, L. & Ahn, Y.S. (1998). Platelet activation in Alzheimer disease. *Arch Neurol.*, Vol. 55, No. 4, (Apr. 1998), pp 530-6, ISSN 0096-6886.
- Shan, Y.; Yu, L.; Li, Y.; Pan, Y.; Zhang, Q.; Wang, F.; Chen, J. & Zhu, X. (2009). Nudel and FAK as antagonizing strength modulators of nascent adhesions through Paxillin. *PLoS Biol.*, Vol. 7, No. 5, (May 2009), pp e1000116, ISSN 1544-9173.
- Shen, Y.; Li, N.; Wu, S.; Zhou, Y.; Shan, Y.; Zhang, Q.; Ding, C.; Yuan, Q.; Zhao, F.; Zeng, R. & Zhu, X. (2008). Nudel binds Cdc42GAP to modulate Cdc42 activity at the leading edge of migrating cells. *Dev. Cell*, Vol. 14, No. 3, (Mar 2008), pp 342-353, ISSN 1534-5807.
- Shockett, P.; Difilippantonio, M.; Hellman, N. & Schatz, D.G. (1995). A modified tetracycline-regulated system provides autoregulatory, inducible gene expression in cultured cells and transgenic mice. *Proc Natl Acad Sci U S A.*, Vol. 92, No. 14, (Jul 1995), pp 6522-6, ISSN 0027-8424.
- Solerte, S.B.; Ceresinib, G.; Ferraria, E. & Fioravantia, M. (2000). Hemorheological changes and overproduction of cytokines from immune cells in mild to moderate dementia of the Alzheimer's type: adverse effects on cerebrovascular system. *Neurobiology of Aging*, Vol. 21, No. 2, (Mar-Apr 2000), pp 271-281, ISSN 0197-4580.
- Sun, X.; Sato, S.; Murayama, O.; Murayama, M.; Park, J.M.; Yamaguchi, H. & Takashima, A. (2002). Lithium inhibits amyloid secretion in COS7 cells transfected with amyloid precursor protein C100. *Neurosci. Lett.*, Vol. 321, No. 1-2, (Mar 2002), pp 61-64, ISSN 0304-3940.
- Tanzi, R.E. (1999). A genetic dichotomy model for the inheritance of Alzheimer's disease and common age-related disorders. *J. Clin. Invest.*, Vol. 104, No. 9, (Nov 1999), pp 1175-1179, ISSN 0021-9738.
- Walsh, D.M.; Minogue, A.M.; Frigerio, C.S.; Fadeeva, J.V.; Wasco, W. & Selkoe, D.J. (2007). The APP family of proteins: similarities and differences. *Biochemical Society Transactions*, Vol. 35, Pt 2, (Apr 2007), pp 416-420, ISSN 0300-5127.

- Wang, H.-Y.; Lee, D.H.S.; Davis, C.B. & Shank, R.P. (2000). Amyloid peptide Abeta 1-42 binds selectively and with picomolar affinity to alpha7 nicotinic receptors. *J. Neurochem.*, Vol. 75, No. 3, (Sep 2000), pp 1155-1161, ISSN 0022-3042.
- Wei, D.Q.; Sirois, S.; Du, Q.S.; Arias, H.R. & Chou, K.C. (2005). Theoretical studies of Alzheimer's disease drug candidate [(2,4-dimethoxy) benzylidene]-anabaseine dihydrochloride (GTS-21) and its derivatives. *Biochem. Biophys. Res. Commun.*, Vol. 338, No. 2, (Dec 2005), pp 1059-1064, ISSN 0006-291X.
- Whitehouse, P.J.; Price, D.L.; Struble, R.G.; Clark, A.W.; Coyle, J.T. & DeLong, M.R. (1982). Alzheimer's disease and senile dementia: loss of neurons in the basal forebrain. *Science*, Vol. 215, No. 4537, (Mar 1982), pp 1237-1239, ISSN 0036-8075.
- Yan, X.; Li, F.; Liang, Y.; Shen, Y.; Zhao, X.; Huang, Q.; & Zhu, X. (2003) Human Nudel and NudE as Regulators of Cytoplasmic Dynein in Poleward Protein Transport along the Mitotic Spindle. *Mol. Cell. Biol.*, Vol. 23, No. 4, (Feb 2003), pp 1239-50, ISSN 0270-7306.
- Yang, F.; Moss, L.G. & Phillips, G.N. Jr. (1996). The molecular structure of green fluorescent protein. *Nat. Biotechnol.*, Vol. 14, No. 10, (Oct 1996), pp 1246-1251, ISSN 1087-0156.
- Yang, J.; Yao, J.; Chen, J.; Wang, X.N.; Zhu, T.Y.; Chen, L.L. & Chu, P. (2009). Construction of drug screening cell model and application to new compounds inhibiting FITC-fibrinogen binding to CHO cells expressing human alphaIIb beta3. *European Journal of Pharmacology*, Vol. 618, No. 1-3, (Sep 2009), pp 1-8, ISSN 0014-2999.
- Yang, J.B.; Yao, J.; Chen, L.L. & Yang, J. (2006). The Amino-Terminal Domain of Integrin beta3 Functions as a Transcriptional Activator in Yeast. *Molecular and Cellular Biochemistry*, Vol. 288, No. 1-2, (Jan 2006), pp 1-5, ISSN 0300-8177.
- Yang, J.B.; Yao, J.; Yang, K.; Hua, Z.C. & Yang, J. (2005). Expression, Purification and Activity Assay of new recombinant antagonists of fibrinogen receptor. *Am. J. Biochem. Biotech.*, Vol. 1, No. 2, (Feb 2005), pp 69-73, ISSN 1553-3468.
- Yang, Z.; Guo, J.; Li, N.; Qian, M.; Wang, S. & Zhu, X. (2003). Mitosin/CENP-F is a conserved kinetochore protein subjected to cytoplasmic dynein-mediated poleward transport. *Cell Res.*, Vol. 13, No. 4, (Aug 2003), pp 275-283, ISSN 1001-0602.
- Yang, J. & Quail, J.W. (1999). Structure of the *Rhizomucor miehei* aspartic proteinase complexed with the inhibitor pepstatin A at 2.7 Å resolution. *Acta Crystallogr., Sect. D*, Vol. 55, No. Pt 3, (Mar 1999), pp 625-630, ISSN 0907-4449.
- Zhang, Q.; Wang, F.; Cao, J.; Shen, Y.; Huang, Q.; Bao, L. & Zhu, X. (2009). Nudel promotes axonal lysosome clearance and endo-lysosome formation via dynein-mediated transport. *Traffic*, Vol. 10, No. 9, (May 2009), pp 1337-1349, ISSN 1600-0854.
- Zhang, H. & Koo, E.H. (2006). The amyloid precursor protein: beyond amyloid. *Molecular Neurodegeneration*, Vol. 1, No. 1, (Jan 2006), pp 5-12, ISSN 1750-1326.
- Zhang, L.; Song, L.; Terracina, G.; Liu, Y.; Pramanik, B. & Parker, E. (2001). Biochemical characterization of the gamma-secretase activity that produces beta-amyloid peptides. *Biochemistry*, Vol. 40, No. 16, (Apr 2001), pp 5049-5055, ISSN 0006-2960.
- Zhou, X.; Wang, R.; Fan, L.; Li, Y.; Ma, L.; Yang, Z.; Yu, W.; Jing, N. & Zhu, X. (2005). Mitosin/CENP-F as a negative regulator of activating transcription factor-4. *J. Biol. Chem.*, Vol. 280, No. 14, (Apr 2005), pp 13973-13977, ISSN 0021-9258.
- Zhu, X. (1999). Structural requirements and dynamics of mitosin-kinetochore interaction in M phase. *Mol. Cell. Biol.*, Vol. 19, No. 2, (Feb 1999), pp 1016-1024, ISSN 0270-7306.
- Zhu, X.; Ding, L. & Pei, G. (1997). Carboxyl terminus of mitosin is sufficient to confer spindle pole localization. *J. Cell. Biochem.*, Vol. 66, No. 4, (Sep 1997), pp 441-449, ISSN 0730-2312.



Advanced Understanding of Neurodegenerative Diseases

Edited by Dr Raymond Chuen-Chung Chang

ISBN 978-953-307-529-7

Hard cover, 442 pages

Publisher InTech

Published online 16, December, 2011

Published in print edition December, 2011

Advanced Understanding of Neurodegenerative Diseases focuses on different types of diseases, including Alzheimer's disease, frontotemporal dementia, different tauopathies, Parkinson's disease, prion disease, motor neuron diseases such as multiple sclerosis and spinal muscular atrophy. This book provides a clear explanation of different neurodegenerative diseases with new concepts of understand the etiology, pathological mechanisms, drug screening methodology and new therapeutic interventions. Other chapters discuss how hormones and health food supplements affect disease progression of neurodegenerative diseases. From a more technical point of view, some chapters deal with the aggregation of prion proteins in prion diseases. An additional chapter to discuss application of stem cells. This book is suitable for different readers: college students can use it as a textbook; researchers in academic institutions and pharmaceutical companies can take it as updated research information; health care professionals can take it as a reference book, even patients' families, relatives and friends can take it as a good basis to understand neurodegenerative diseases.

How to reference

In order to correctly reference this scholarly work, feel free to copy and paste the following:

Xiao-Ning Wang, Jie Yang, Ping-Yue Xu, Jie Chen, Dan Zhang, Yan Sun and Zhi-Ming Huang (2011). Construction of Drug Screening Cell Model and Application to New Compounds Interfering Production and Accumulation of Beta-Amyloid by Inhibiting Gamma-Secretase, Advanced Understanding of Neurodegenerative Diseases, Dr Raymond Chuen-Chung Chang (Ed.), ISBN: 978-953-307-529-7, InTech, Available from: <http://www.intechopen.com/books/advanced-understanding-of-neurodegenerative-diseases/construction-of-drug-screening-cell-model-and-application-to-new-compounds-interfering-production-an>

INTECH
open science | open minds

InTech Europe

University Campus STeP Ri
Slavka Krautzeka 83/A
51000 Rijeka, Croatia
Phone: +385 (51) 770 447
Fax: +385 (51) 686 166

InTech China

Unit 405, Office Block, Hotel Equatorial Shanghai
No.65, Yan An Road (West), Shanghai, 200040, China
中国上海市延安西路65号上海国际贵都大饭店办公楼405单元
Phone: +86-21-62489820
Fax: +86-21-62489821

www.intechopen.com

IntechOpen

IntechOpen

© 2011 The Author(s). Licensee IntechOpen. This is an open access article distributed under the terms of the [Creative Commons Attribution 3.0 License](https://creativecommons.org/licenses/by/3.0/), which permits unrestricted use, distribution, and reproduction in any medium, provided the original work is properly cited.

IntechOpen

IntechOpen